Capillary forces and structuring in layers of colloid particles

Peter A. Kralchevsky*, Nikolai D. Denkov

Laboratory of Chemical Physics and Engineering, Faculty of Chemistry, University of Sofia, 1 James Bourchier Avenue, Sofia 1164, Bulgaria

Abstract

‘Capillary forces’ are interactions between particles mediated by fluid interfaces. Recent advances in this field have been achieved by experiments and theory on lateral capillary forces, which are due to the overlap of menisci formed around separate particles attached to an interface. In particular, we should mention the cases of ‘finite menisci’ and ‘capillary multipoles’. The capillary-bridge forces were investigated in relation to capillary condensation and cavitation, surface-force measurements and antifoaming by oily drops. The studies on colloidal self-assembly mediated by capillary forces developed in several promising directions. The obtained structures of particles have found numerous applications. © 2001 Elsevier Science Ltd. All rights reserved.

Keywords: Capillary interactions; Lateral capillary forces; Capillary bridges; Colloidal self-assembly; Arrays of particles; Particulate monolayers

1. Introduction

In general, we call ‘capillary forces’ interactions between particles, which are mediated by fluid interfaces. The interest in these forces has grown due to their recognised importance for the self-assembly of macroscopic and microscopic (Brownian) particles and even of protein molecules and viruses [1–3•].

In some cases, the liquid phase forms a capillary bridge between two particles or bodies. Then the capillary force is directed *normally* to the planes of the contact lines on the particle surfaces (Fig. 1a). The normal capillary-bridge forces can be attractive or repulsive depending on whether the capillary bridge is concave or convex. Attractive forces of this type lead to 3D (three-dimensional) aggregation and consolidation of bodies built up from particulates. A spontaneous formation of sub-micrometer gas-filled capillary bridges in water seem to be the most probable explanation of the hydrophobic surface force.

In other cases, each individual particle causes some perturbation in the shape of a liquid interface or film. The overlap of the perturbations (menisci) around two particles gives rise to a *lateral* capillary force between them (Fig. 1b,c,d,e). This force could be attractive or repulsive depending on whether the overlapping menisci, formed around the two particles, are similar (say, both concave) or dissimilar (one is concave and the other is convex). The attractive lateral capillary forces cause 2D (two-dimensional) aggregation and ordering in a rather wide scale of particle sizes: from 1 cm down to 1 nm.

Below we first briefly review recent publications on capillary forces. Next we shortly discuss studies in which structuring under the action of lateral capillary
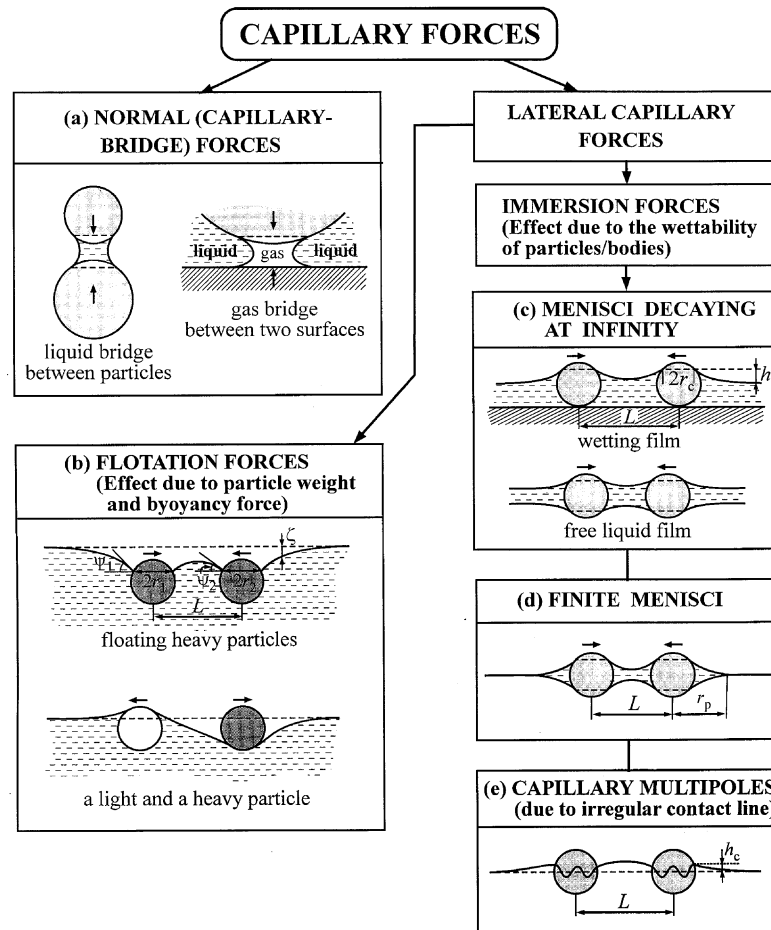

Fig. 1. Types of capillary forces: (a) The *normal* capillary forces can be due to either liquid-in-gas or gas-in-liquid capillary bridges, which lead to particle–particle and particle–wall interactions, the force is directed normally to the contact line. In the case of *lateral* capillary forces (b,c,d,e) the force is parallel to the contact line. The interaction is due to the overlap of interfacial deformations created by the separate particles. (b) In the case of *flotation* force the deformations are caused by the particle weight and buoyancy. In the case of *immersion* forces (c,d,e) the deformations are related to the wetting properties of the particle surface: position and shape of the contact line; and magnitude of the contact angle. When the deformation around an isolated particle is axisymmetric, we deal with '*capillary charges*', one can distinguish cases of infinite (c) and finite (d) menisci, see Eqs. (5) and (14). (e) The forces between particles of undulated or irregular contact line can be described as interactions between '*capillary multipoles*', in analogy with electrostatics; see Eq. (15).

forces is reported. Comprehensive reviews on capillary forces and particle structuring can be found in Kralchevsky and Nagayama 2000, 2001 [2•,3•].

2. Normal (capillary-bridge) force

2.1. Definition, measurements and physical importance

Here we summarise the most important information and briefly review recent publications on capillary-bridge forces. A detailed review can be found in Chapter 11 of Kralchevsky and Nagayama 2001 [3•].

The presence of a liquid bridge between two solid surfaces (Fig. 1a) leads to their interaction through a capillary force, F_c, owing to the pressure difference across the curved interface and the action of the

surface tension force exerted around the annulus of the meniscus:

$$F_c = -\pi(2r\sigma\sin\theta - r^2 P_c) \qquad (0 \leq \theta \leq \pi) \qquad (1)$$

Here σ is the surface (interfacial) tension, P_c is the difference between the pressures inside and outside the bridge (the capillary pressure), r and θ are the radial coordinate and the meniscus slope angle corresponding to an arbitrary cross-section of the meniscus. For example, $\theta = \pi/2$ for a section across the neck of a bridge and then Eq. (1) can be presented in the form $F_c = -2\pi\sigma r_0 (1-p)$, where r_0 is the radius of the neck and $p = P_c r_0/2\sigma$ is the dimensionless capillary pressure. In general, $-\infty < p < +\infty$. According to the classification of Plateau, with the increase of p the shape of the capillary bridge becomes, con-

secutively, concave nodoid $(-\infty < p < 0)$, catenoid $(p = 0)$, concave unduloid $(0 < p < 1/2)$, cylinder $(p = 1/2)$, convex unduloid $(1/2 < p < 1)$, sphere $(p = 1)$ and convex nodoid $(1 < p < +\infty)$. For $p < 1$ the capillary-bridge force is attractive $(F_c < 0)$, whereas for $p > 1$ it becomes repulsive $(F_c > 0)$; for a bridge with spherical meniscus we have $F_c = 0$.

The effect of capillary bridges is essential for the assessment of the water saturation in soils and the adhesive forces in any moist unconsolidated porous media, for the dispersion of pigments and wetting of powders, for the adhesion of dust and powder to surfaces, for flocculation of particles in three-phase slurries, for liquid-phase sintering of fine metal and polymer particles, for obtaining of films from latex and silica particles, for calculation of the capillary evaporation and condensation in various porous media, for estimation of the retention of water in hydrocarbon reservoirs and for granule consolidation [3•].

The action of capillary-bridge force is often detected in experiments with atomic force microscopy (AFM) [4–6]. For example, Fujihira et al. [4] used AFM as a friction-force microscope. At higher humidity in the atmosphere they detected a higher friction, which was attributed to the presence of an aqueous bridge due to capillary condensation.

AFM was also used to measure the interaction between a small solid spherical particle and a gas bubble attached to a substrate [7–10•,11]. In fact, after the particle enters the air–liquid interface, the bubble plays the role of a gaseous capillary bridge between the particle and the substrate. The measured capillary-bridge force is non-monotonic and depends considerably on the three-phase contact angle [7]. In some experiments a hysteresis of the contact angle was detected; from the measured capillary force one can determine the advancing and receding contact angles on individual particles and to check whether there is hysteresis [8–10•].

Capillary bridges between two fluid phases are found to play an important role in the process of antifoaming by dispersed oil drops [12–14•,15]. When an oil droplet bridges between the surfaces of an aqueous film, two scenarios of film destruction are proposed: (i) dewetting of the droplet could cause film rupture; and (ii) the formed oil bridge could have an unstable configuration and the film could break at the centre of the expanding destabilised bridge. The latter mechanism was recorded experimentally with the help of a high-speed video camera [13] and the results were interpreted in terms of the theory of capillary-bridge stability [14•].

2.2. Theoretical calculations of the capillary-bridge force

To calculate F_c for a given configuration of the capillary bridge one can use Eq. (1), along with some appropriate expressions for the meniscus shape. The contact angle, contact radius and the radius of the neck are connected by simple analytical expressions, see equations 11.35–11.38 in Kralchevsky and Nagayama [3•]. The profile, surface area and volume of a bridge can be expressed in terms of elliptic integrals, see Table 11.1 in Kralchevsky and Nagayama [3•]. The elliptic integrals can be computed by means of the stable numerical methods of 'arithmetic–geometric mean', see Chapter 17.6 in Abramowitz and Stegun [16]. Alternatively, the Laplace equation of capillarity can be solved numerically to determine the shape of the bridge and the capillary pressure. For example, in this way Dimitrov et al. [17] estimated the capillary forces between silica particles in amorphous monolayers. Likewise, Aveyard et al. [18] calculated the liquid bridge profile in a study of the effects of line tension and surface forces on the capillary condensation of vapours between two solid surfaces.

Various approximate expressions for F_c are available for pendular rings, that is a liquid capillary bridge formed around the point at which a spherical particle of radius R touches a planar surface (plate). If the radii of the contact lines are much smaller than R, one can use the formula derived by Orr et al. [19]:

$$F_c \approx -2\pi\sigma R(\cos\theta_1 + \cos\theta_2) \qquad (2)$$

where θ_1 and θ_2 are the contact angles at the surfaces of the particle and the plate. If the radii of the contact lines are not much smaller than R, one can use several alternative expressions for F_c, all of them derived in the framework of the so called 'toroid' or 'circle' approximation: the generatrix of the bridge surface is approximated with a circumference, see equations 11.11–11.13 in Kralchevsky and Nagayama [3•]. Using the same approximation, de Lazzer et al. [20] derived analytical expressions for F_c for the cases when the particles are spherical, paraboloidal or conical. The obtained formulas were verified against the respective exact computer solutions.

Kolodezhnov et al. [21] derived a set of equations which provide a convenient way to compute the shape of the capillary bridge between two identical spherical particles and to calculate F_c. At the last step numerical solution was used. The accuracy of the circle approximation was verified against the exact solution for various values of the system parameters. In addition, an approximate relationship between the capillary force and the moisture of a powder was derived [21]. Willett et al. [22] obtained closed-form approximated expressions for the capillary-bridge force between equal and unequal spheres as a function of the separation distance and for a given bridge volume and contact angle. These authors developed also a

method for measuring the capillary forces arising from microscopic pendular liquid bridges. The experimental force-vs.-distance curves were found to agree excellently with the respective theoretical dependencies calculated by numerical integration of the Laplace equation [22].

2.3. Nucleation of bridges: capillary condensation and cavitation

If the length of a capillary bridge is gradually increased, the bridge becomes unstable and ruptures at a given critical (maximum) length. Conversely, if the distance between two approaching parallel hydrophilic plates in humid atmosphere becomes smaller than the maximum length of the stable water bridges, then such bridges can spontaneously appear due to 'capillary condensation' of vapours. Likewise, if the distance between two parallel hydrophobic plates in water is smaller than the maximum length of the stable vapour-filled bridges, then such bridges can appear owing to a spontaneous cavitation due to fluctuational formation and growth of critical bridges−nuclei [3•]. The maximum length, h_{max}, of a stable nodoid-shaped bridge can be estimated by means of the asymptotic expression:

$$h_{max} = \frac{2\sigma\cos\varphi_c}{|P_c|} \qquad (70° < \varphi_c < 90°) \qquad (3)$$

see equations 11.76−11.78 in Kralchevsky and Nagayama [3•], φ_c is the contact angle measured across the bridge phase; for φ_c out of the above interval a more complicated expression for h_{max} is to be used. For a bridge, which is in chemical equilibrium with the ambient mother phase, one has:

$$|P_c| = \begin{cases} P - P_0 \text{ for vapor-filled bridge} \\ (kT/V_m)\ln(P_0/P') \text{ for liquid bridge} \end{cases} \qquad (4)$$

Here P is the outer (usually the atmospheric) pressure, P_0 is the equilibrium vapour pressure of the liquid and P' is the partial pressure of the vapours in the ambient gas phase, V_m is the volume per molecule in the liquid phase, k is the Boltzmann constant and T is temperature. For example, taking $P = 1$ atm, contact angle $\theta = 90° - \varphi_c = 94°$, $\sigma = 72.75$ mN/m and $P_0 = 2337$ Pa from Eqs. (3) and (4) one calculates $h_{max} = 103$ nm for a vapour-filled bridge between two parallel hydrophobic plates in water at 20°C. Note that the latter estimate holds for degassed (deaerated) water. The presence of dissolved gas much facilitates the cavitation. In such cases the shape of the capillary bridge could be approximated with a cylinder [23], instead of considering a concave nodoid.

Capillary bridging between two glass surfaces in a humid atmosphere was observed by Yaminsky [24]; the formation of a water bridge by capillary condensation was detected as a discontinuity in the force−distance dependence. Xiao and Qian [25] investigated, by AFM, the dependence of the capillary-bridge force on humidity. In the case of less hydrophilic surfaces they detected an adhesive force, which is independent of humidity and in agreement with Eq. (2). In contrast, between more hydrophilic surfaces (enhanced capillary condensation) these authors measured a humidity-dependent capillary-bridge force. The latter means that the simplifying assumptions used to derive Eq. (2) are not satisfied and more complicated theoretical expressions have to be applied to interpret the data [25].

Capillary condensation of water bridges was established not only when the ambient mother phase is a humid atmosphere, but also when this phase is oil [26] and even — a bicontinuous microemulsion [27]. With the help of a surface force apparatus, Claesson et al. [26] detected capillary bridging between mica surfaces immersed in triolein, which had been pre-equilibrated with water. With a similar technique Petrov et al. [27] measured the force between two mica surfaces immersed in a microemulsion (AOT/decane/brine). A contribution of capillary bridge-forces was detected and the force profile was experimentally obtained on both approach and separation.

As already mentioned, the capillary-bridge force is one of the major candidates for explanation of the attractive hydrophobic surface force. Gaseous bridges could appear even if there is no dissolved gas in the water phase. The pressure inside a bridge can be as low as the equilibrium vapour pressure of water owing to the high interfacial curvature of nodoid-shaped bridges, see Eqs. (3) and (4) above. Alternatively, the gas bridges could be formed by merging of two bubbles attached to the two opposite approaching surfaces. A number of recent studies [23,26−35] provided evidence in support of the capillary-bridge origin of the long-range hydrophobic surface force. In particular, the observation of 'steps' in the experimental data was interpreted as an indication for separate acts of bridge nucleation or coalescence of attached bubbles [23]. Both mechanisms are possible; for example the more difficult bridging upon the first contact of two hydrophobic surfaces [32] can be attributed to nucleation, whereas the easier bridging upon the second, third, etc. contacts could be due to the coalescence of residual attached bubbles obtained after destruction of the initial bridge. The experiments by Ederth [33] show that the hydrophobic attraction becomes more pronounced during the process of an experiment, because gases from the air dissolve into the originally

degassed water, resulting in an easier capillary bridging when the surfaces approach each other. Indications about the existence of nano-bubbles attached to a hydrophobic surface were established by means of AFM experiments [35]. It is still unclear why the gas in such bubbles does not dissolve in the surrounding water in view of their high surface curvature which produces a great internal pressure.

3. Lateral capillary forces

3.1. Theoretical background

First we briefly consider the theoretical aspects of the lateral capillary forces, following references by Kralchevsky and Nagayama [2•,3•]. The applied aspects, related to 2D structuring of particles, are reviewed in subsequent sections.

As mentioned in the introduction, the origin of the lateral capillary forces is the overlap of perturbations in the shape of a liquid surface due to the presence of attached particles. The larger the interfacial deformation created by the particles, the stronger the capillary interaction between them. It is known that two similar particles floating on a liquid interface attract each other (Fig. 1b). This attraction appears because the liquid meniscus deforms in such a way that the gravitational potential energy of the two particles decreases when they approach each other. Hence the origin of this *flotation* capillary force is the particle weight (including the Archimedes force). Capillary interaction appears also when the particles (instead of being freely floating) are partially immersed (confined) in a liquid layer; this is the *immersion* capillary force (Fig. 1c,d). The deformation of the liquid surface in this case is related to the wetting properties of the particle surface, i.e. to the position of the contact line and the magnitude of the contact angle, rather than to gravity. The flotation and immersion forces can be attractive or repulsive.

For the systems depicted in Fig. 1b,c (menisci decaying at infinity), solving the Laplace equation of capillarity for small meniscus slope, $\nabla^2 \zeta = q^2 \zeta$, in cylindrical coordinates (r, φ), one can determine the interfacial shape around a single particle:

$$\zeta(r) = A K_0(qr) \qquad (5)$$

where K_0 is the modified Bessel function of the second kind and zeroth order and A is a constant of integration,

$$q^2 = \Delta\rho g / \sigma \quad \text{(for thick films)}$$
$$q^2 = (-\Pi') / \sigma \quad \text{(for thin films)} \qquad (6)$$

Here $\Delta\rho$ is the difference between the mass densities of the two fluids, g is the acceleration due to gravity and Π' is the derivative of the disjoining pressure with respect to the film thickness. Eq. (5) describes a meniscus which is exponentially decaying at infinity. Furthermore, one can apply the superposition approximation, i.e. assume that the interfacial deformation caused by two particles (Fig. 1b,c) is equal to the sum of the deformations caused by the separate particles in isolation. Then, in view of Eq. (5), the energy of lateral capillary interaction between the two particles is obtained in the form [2•,3•,36]:

$$\Delta W \approx -2\pi\sigma Q_1 Q_2 K_0(qL) \qquad (7)$$

where L denotes the distance between the centres of the two particles, $Q_i \equiv r_i \sin\psi_i$ $(i = 1,2)$ are the so-called 'capillary charges', r_i and ψ_i are the radii of the contact line and the slope angle at the contact line of the respective particle (see Fig. 1b for the notation). ΔW represents a variation in the gravitational energy in case of flotation force, or in the energy of wetting in case of immersion force. The lateral capillary force is given by the derivative $F = -d\Delta W/dL$, which yields:

$$F \approx -2\pi\sigma Q_1 Q_2 q K_1(qL), \qquad (r_k \ll L) \qquad (8)$$

(K_1 — modified Bessel function). The asymptotic form of Eq. (8) for $qL \ll 1$ ($q^{-1} = 2.7$ mm for water):

$$F = -2\pi\sigma Q_1 Q_2 / L, \qquad (r_k \ll L \ll q^{-1}) \qquad (9)$$

looks like a two-dimensional analogue of Coulomb's law for the electric force. This is the reason for calling Q_1 and Q_2 'capillary charges'. Generally speaking, the capillary charge characterises the local deviation of the meniscus shape from planarity at the three-phase contact line. The flotation and immersion capillary forces exhibit similar dependence on the interparticle separation, L, but very different dependencies on the particle radius and the surface tension of the liquid. The different physical origin of these forces results in different magnitudes of the corresponding 'capillary charges'. In this respect there is an analogy with the electrostatic and gravitational forces, which obey the same power law, but differ in the physical meaning and magnitude of the force constants (charges, masses). In this particular case, when $R_1 = R_2 = R$ and $r_k \ll L \ll q^{-1}$, one can derive [2•,3•]:

$$F \propto (R^6 / \sigma) K_1(qL) \quad \text{for flotation force}$$
$$F \propto \sigma R^2 K_1(qL) \qquad \text{for immersion force} \qquad (10)$$

In other words, the flotation force decreases, while the immersion force increases, when the interfacial tension σ increases. Besides, the flotation force decreases with the decrease of R much more strongly than the immersion force. Thus, the flotation force is negligible for $R < 5 - 10 \ \mu$m, whereas the immersion force can be significant even when $R = 2$ nm. The latter force is one of the main factors causing the self-assembly of small colloidal particles and protein macromolecules confined in thin liquid films or lipid bilayers; see Kralchevsky and Nagayama [2•,3•] for details.

The analogy between the capillary and electrostatic interactions was discussed in more details by Paunov [37]. This analogy can be extended further: in addition to the immersion force between 'capillary charges' (monopoles), one can also examine immersion forces between 'capillary multipoles', see below.

3.2. Flotation capillary forces

Here we briefly describe some specific and recent results for the flotation forces. The 'capillary charge' for floating particles can be estimated from the expression [3•,36]

$$Q_i \approx \frac{1}{6}q^2R_i^3(2 - 4D_i + 3\cos\alpha_i - \cos^3\alpha_i),$$
$$(i = 1,2) \tag{11}$$

where $D_i = (\rho_i - \rho_{II})/(\rho_I - \rho_{II})$, ρ_i, ρ_I and ρ_{II} are the mass densities of the particle and lower and upper fluid phases, respectively. Eq. (11) allows one to calculate the capillary charge Q_i directly from the particle radius R_i and three-phase contact angle α_i. The convenient asymptotic expressions, Eqs. (8) and (11), can be used to calculate the flotation capillary force for $qR_i \ll 1$ and $L > 4R_i$. In all other cases one could apply a more accurate computational procedure, which is described in section 8.1.5 of Kralchevsky and Nagayama [3•].

If a vertical plate is partially immersed in a liquid, a capillary meniscus is formed in a vicinity of the plate (wall). The overlap of the latter meniscus with the meniscus around a floating particle gives rise to a capillary force (particle–wall interaction), which is described by equation 8.106 in Kralchevsky and Nagayama [3•]. If a particle slides along an inclined meniscus, for small Reynolds numbers the capillary force is completely counterbalanced by the hydrodynamic drag force and then the velocity of particle motion is proportional to the capillary force [38]. The coefficient of proportionality gives the hydrodynamic drag coefficient, f_d, which turns out to be dependent on the type of surfactant and the density of its adsorption layer at the interface. Petkov et al. [38] developed

a 'sliding particle' method for determining the coefficient of surface shear viscosity of surfactant adsorption monolayers from the measured f_d. Similar experimental method was applied to measure the yield stress of protein adsorption layers, which exhibit elastic and plastic behaviour [39].

Whitesides et al. [40–42] investigated in detail the self-assembly of mesoscale objects under the action of lateral capillary forces. In the case of heavy (or light) particles, the flotation capillary force was responsible for the observed interparticle attraction. To estimate the force per unit area of the particle contact line these authors applied the Laplace equation for a meniscus of translational symmetry [40–42]. In some of the studies they used floating hexagonal plates of alternatively changing hydrophobic and hydrophilic edges (sides) [41••]. In such cases, the immersion force between capillary multipoles, in conjunction with the flotation force, is responsible for the observed self-assembly (Section 3.4).

3.3. Immersion force between 'capillary charges'

As already mentioned, in the case of the immersion force the interfacial deformation is related to the wetting properties of the particle surface (position and shape of the contact line and magnitude of the contact angle), rather than to particle weight and buoyancy, Fig. 1c. The asymptotic Eq. (8) can be used to calculate the immersion force only for large interparticle distance L, for which the 'capillary charges' $Q_i \equiv r_i \sin \psi_i$ are independent of L. However, for shorter distances both r_i and ψ_i become functions of L, in such cases one can calculate the immersion capillary force using the procedure described in section 7.3.2 of Kralchevsky and Nagayama [3•]. There one can find computational procedures for various configurations: two spherical particles; two vertical cylinders; sphere and cylinder; sphere and vertical wall, etc. In addition, two types of boundary conditions are considered: (i) fixed contact angle; and (ii) fixed contact line, which affects the magnitude of the immersion capillary force; see section 7.3.4 in Kralchevsky and Nagayama [3•]. In particular, if the position (elevation) of the contact line is fixed at the particle surface, i.e. $z = h_c = $ const., then the energy of capillary interaction between two equal particles of circular contact lines of radius r_c (Fig. 1c) is given by the expression [43]:

$$\Delta W(L) = 2\pi\sigma q r_c h_c^2 \left[\frac{K_1(qr_c) - \frac{1}{2}qr_c K_0(qL)}{K_0(qr_c) + K_0(qL)} \right.$$
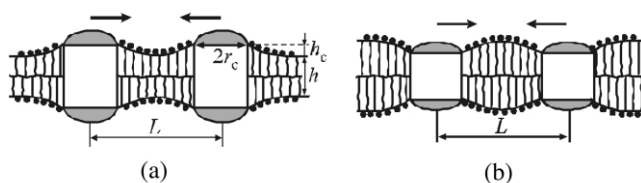
Fig. 2. The hydrophobic thickness of an inclusion (transmembrane protein) can be (a) greater or (b) smaller than the thickness, h, of the non-disturbed phospholipid bilayer. The overlap of the deformations around two similar inclusions gives rise to attraction between them [3●,43]. The interaction energy can be estimated by means of Eq. (12), h_c is the mismatch between the hydrophobic thicknesses of the inclusion and bilayer.

$$- \frac{K_1(qr_c)}{K_0(qr_c)} \Bigg] \qquad (12)$$

where q is defined by Eq. (6) for liquid interfaces or films. Eq. (12) can also be applied to describe the energy of interaction between two inclusions (for instance membrane proteins) in a bilayered lipid membrane. In the latter case $q \approx [4\lambda/(h\sigma)]^{1/2}$, where λ is the shear elastic modulus in the hydrocarbon-chain zone and h is its thickness (Fig. 2), for details see Kralchevsky et al. [43] and Chapter 10 in Kralchevsky and Nagayama [3●]. Note that the interaction energy, as given by Eq. (12), is proportional to h_c^2, i.e. to the squared mismatch between the hydrophobic zones of the inclusion and bilayer. This interaction can be one of the reasons for aggregation of membrane proteins in biomembranes [43–45].

The immersion capillary force can also be operative between particles captured in a spherical (rather than planar) thin liquid film or lipid vesicle [3●,46]. In this case the 'capillary charge' characterises the local deviation of the meniscus shape from sphericity (rather than from planarity) at the contact line.

Maenosono et al. [47] examined experimentally the motion of millimetre-sized spheres which are partially immersed in a wetting film (Fig. 1c). Employing Eq. (9) to estimate the immersion force, these authors determined the friction coefficient (related to the drag force) from the data for the particle law of motion $L(t)$, where t is time. It turned out that the friction with the substrate is negligible and the main hydrodynamic resistance comes from the viscous friction in the liquid film [47].

It is worthwhile noting that Eqs. (5)–(9) are valid for menisci decaying at infinity (Fig. 1c). However, it is possible the particle size is much greater than the film thickness, as shown in Fig. 1d. For example, Velikov et al. [48●] observed a strong lateral attraction between latex particles of diameter $2R \approx 7$ μm, entrapped in a foam film of thickness which is at least 100 times smaller. Analogous observations have been

done with micrometer-sized latex spheres encapsulated within the bilamellar membrane of a giant lipid vesicle [49,50●]. These experiments neatly reveal the film deformation caused by the particles and the related attraction between them. For such systems the meniscus profile around a single particle obeys the equation (for small meniscus slope):

$$\sigma \frac{1}{r} \frac{d}{dr}\left(r \frac{d\zeta}{dr}\right) = \Delta P = \text{const.} \qquad (13)$$

where ΔP is the pressure jump across the meniscus. ΔP is constant if the effect of the gravitational hydrostatic pressure is negligible. The general solution of Eq. (13) is:

$$\zeta(r) = A + B\ln r + (\Delta P/4\sigma)r^2 \qquad (14)$$

where A and B are constants of integration. In other words, Eq. (13) has no axisymmetric solution which is finite at infinity ($r \to \infty$), cf. Eqs. (5) and (14). The latter fact implies that the meniscus around a particle must end at a peripheral contact line (of radius r_p), out of which the film is plane-parallel ($\zeta \equiv 0$), see Fig. 1d. Hence, we deal with a 'finite' meniscus. In this case the overlap of the menisci and the interaction between the particles, begins when they are at a distance $L < 2r_p$ from each other. Such types of interaction is obviously different from that described by Eq. (7), which for long distances yields $\Delta W \propto (qL)^{-1/2} \exp(-qL)$.

The problem with the immersion capillary force, F, in the case of finite menisci was examined theoretically in Danov et al. [50●] and in a more detailed article by Danov et al. (Langmuir 2001, submitted). Both the theory and experiment show that in the investigated case F corresponds to attraction, whose magnitude, $|F| = |F(L)|$ has a peculiar non-monotonic behaviour: for short distances $|F|$ increases with L, then $|F|$ has a maximum; and decreases further. Moreover, the capillary interaction exhibits hysteresis: on approach of two particles one has $F = 0$ for $L > 2r_p$, the interaction begins with a jump when the two peripheral contact lines touch each other. In contrast, on separation of the two interacting particles (and of the two overlapping menisci) one has $F \neq 0$ for $L > 2r_p$. With further increases in L the configuration of the meniscus becomes unstable and it splits to two separate menisci around the respective individual particles.

3.4. Immersion forces between 'capillary multipoles'

The weight of a floating micrometer-sized particle is too small to create any surface deformation. However, surface deformations could appear if the contact

line on the particle surface is irregular (say, undulated as in Fig. 1e), rather than a perfect circumference. In this case, instead of Eq. (5), the meniscus shape around a single particle is described by the expression:

$$\zeta(r,\varphi) = \sum_{m=1}^{\infty} K_m(qr)(A_m \cos m\varphi + B_m \sin m\varphi) \quad (15)$$

This equation is the respective solution of the linearized Laplace equation of capillarity for small meniscus slope, $\nabla^2 \zeta = q^2 \zeta$, in cylindrical coordinates (r,φ). Here A_m and B_m are constants of integration. For $qr \ll 1$ one has $K_m(qr) \propto (qr)^{-m}$ and then Eq. (15) reduces to a multipole expansion (a 2D analogue of Eq. (15) in electrostatics). The terms with $m = 1, 2, 3,...$ correspond to 'dipole', 'quadrupole', 'hexapole', etc. In fact, such multipoles were experimentally realised by Bowden et al. [40,41••] by the appropriate hydrophobization or hydrophilization of the sides of floating hexagonal plates.

From a theoretical viewpoint, the capillary force between particles of irregular or undulated contact line is a kind of immersion force insofar as it is related to the particle wettability, rather than to the particle weight. Eq. (5) is the zeroth-order term of the expansion in Eq. (15). For $m \geq 1$ the capillary force can cause not only translation, but also rotation of the particles. Theoretical description of this capillary force was recently given by Stamou et al. [51••] for rough colloidal spheres. These authors note that for freely floating particles the capillary force will spontaneously rotate each particle around a horizontal axis to annihilate the capillary dipole moment. Therefore, the term with $m = 1$ in Eq. (15) has to be skipped and the leading multipole order in the capillary force between such two particles is the quadrupole–quadrupole interaction ($m = 2$); the respective interaction energy is [51••]:

$$\Delta W(L) = -12\pi\sigma h_c^2 \cos(2\varphi_A + 2\varphi_B)\frac{r_c^4}{L^4} \quad (m = 2)$$
$$(16)$$

Here h_c is amplitude of the undulation of the contact line, whose average radius is r_c. The angles φ_A and φ_B are subtended between the diagonals of the respective quadrupoles and the line connecting the centres of the two particles. For two particles in contact ($L/r_c = 2$) and optimal orientation, $\cos(2\varphi_A + 2\varphi_B) = 1$, one obtains $\Delta W = -(3/4)\pi\sigma h_c^2$. Thus, for interfacial tension $\sigma = 35$ mN/m the interaction energy ΔW becomes greater than the thermal energy kT for undulation amplitude $h_c > 2.2$ Å. This result is really astonishing: even a minimal roughness of the

contact line could be sufficient to give rise to a significant capillary attraction, which may produce 2D aggregation of colloidal particles attached to a fluid interface, also see Lucassen [52] and Chapter 12 in Kralchevsky and Nagayama [3•]. However, in the angstrom scale the fluid interfaces are not smooth: they are corrugated by thermally excited fluctuation capillary waves, whose amplitude is typically 3–6 Å. Hence, one can expect that the effect of the contact-line undulations will become significant when their amplitude is greater than the background stochastic noise, that is for nanometre and larger amplitudes [3•].

Note that both Eqs. (12) and (16) give $\Delta W \propto h_c^2$. With respect to the force, $F = -d(\Delta W)/dL$, for the immersion force between two 'capillary charges' (monopoles) we have $F \propto 1/L$, whereas in the case of two quadrupoles the force is $F \propto 1/L^5$. In other words, for $qr \ll 1$, the range of action of the capillary force decreases with the increase of the multipole order, as it could be expected. Consequently, if capillary charges (i.e. multipoles of the lowest order) are present, as a rule they dominate the capillary interaction.

Another difference between the cases of interacting capillary 'charges' and 'multipoles' is that the interaction is isotropic for charges, whereas for multipoles ($m \geq 2$) its sign and magnitude depend on the particle mutual orientation. For that reason, as sketched in Fig. 3a,e, the immersion force between quadrupoles ($m = 2$) will tend to organise them in a square lattice, rather than in a hexagonal one. Particles–hexapoles ($m = 3$) can be arranged into a hexagonal lattice with voids (Fig. 3c), or without voids (Fig. 3b,f). In fact, such lattices (hexagonal with voids and square) have been observed in the experiments of Bowden et al. [40,41••].

The angular dependence of the immersion force between multipoles leads to the conclusion that this force could hardly produce formation of 2D crystals from a mixture of particles with different multipole orders m. In principle, it is possible this capillary interaction is able to induce a 'phase separation' of the mixture into ordered domains of particles with the same m. Another possibility, suggested in reference [51••], is that the particles could form simple linear aggregates. When two or more modes contribute with a considerable weight to the multipole expansion, Eq. (15), the capillary force is expected to be unable to cause two-dimensional crystallisation of the respective particles, because of their inadequate relative orientations [51••].

It is worthwhile noting that Lucassen [52] was the first who developed a quantitative theory of the capillary forces between particles with an undulated contact line. He considered 'rough-edged' cubic particles
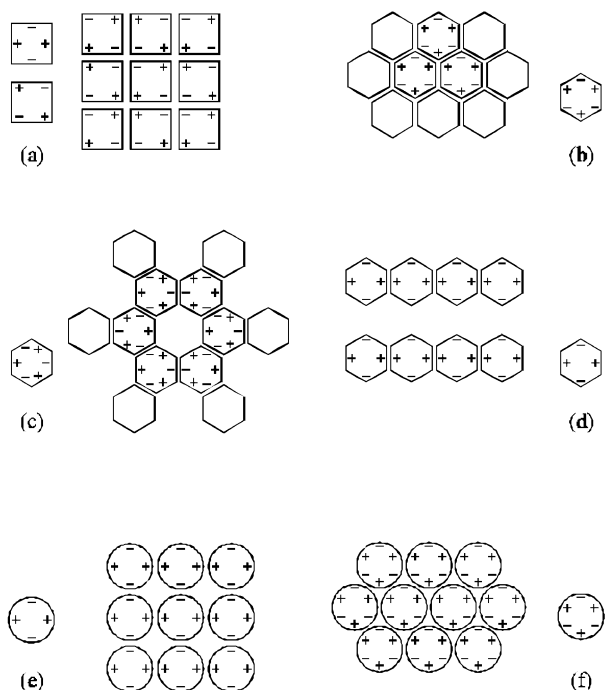
Fig. 3. The 2D arrays formed by capillary quadrupoles ($m = 2$) and hexapoles ($m = 3$) [41$^{\bullet\bullet}$,51$^{\bullet\bullet}$]; the signs '+' and "−" denote, respectively, positive and negative 'capillary charges', i.e. convex and concave local deviations of the meniscus shape from planarity at the contact line. (a) Quadrupoles of square shape form tetragonal close-packed array, irrespectively of the location of the capillary charges (on the sides or on the corners of the square). (b) Plates with a hexagonal shape form a close-packed array only if the charges are located on the corners, whereas (c) porous (opened) hexagonal array is formed when the charges are located on the hexagon sides. (d) Quadrupoles having the shape of hexagons form linear aggregates [51$^{\bullet\bullet}$]. (e) Quadrupoles having circular shape will form square array, (f) circular hexapoles can form close-packed hexagonal array. Note that the aggregate structure depends on both the distribution of the capillary charges and the geometrical shape of the elementary cell.

with a sinusoidal contact line. The calculated capillary force exhibits a minimum: it is attractive at long distances and repulsive at short separations. Any interfacial deformation, either by dilatation or by shear, will take the particles out of their equilibrium positions (at the minimum) and will, therefore, be resisted. As a consequence, the particulate monolayer will exhibit dilatational and shear elastic properties [52]. The respective surface dilatational and shear elastic moduli can be estimated by means of the expressions [3$^{\bullet}$]:

$$E_{dil} \approx \frac{2\pi^3 \sigma h_c^3}{\lambda^2 \Delta h_c}, \qquad E_{sh} \approx 2\pi^2 \sigma \frac{h_c^2}{\lambda^2} \qquad (17)$$

where λ is the wavelength of the undulations, h_c is their average amplitude and Δh_c is the standard deviation of the amplitude from its mean value. It is assumed that $\Delta h_c \ll h_c$ and that the length of the

edge of the cubic particles is equal to λ. With $\sigma = 40$ mN/m, $\lambda = 1$ μm, $h_c = 100$ nm and $\Delta h_c = 20$ nm Eq. (17) yields $E_{dil} \approx 124$ mN/m and $E_{sh} \approx 8$ mN/m. The latter values of the surface elasticities are comparable with those for protein adsorption layers [53]. However, the predictions of Eq. (17) have not yet been verified experimentally.

4. Self-assembly of particles under the action of capillary forces

4.1. Assembly of spherical particles in wetting films

The process of formation of well ordered 2D particle arrays in evaporating wetting films was known for many years [54−59]. Regular arrays of latex particles were often fabricated by evaporation of drops of suspensions on solid substrates to prepare samples for optical studies [54] or for modelling the process of paint drying [55]. In the 1970s the 'mica spreading technique' was introduced for preparation of 2D crystals of viruses and proteins [56,57], which were suitable for structural analysis by electron microscopy. Yoshimura et al. [58], developed a mercury spreading technique and obtained 2D crystals from a dozen of protein [3$^{\bullet}$,59].

The mechanism and the governing forces of the 2D particle assembly in evaporating wetting films were clarified about a decade ago [60,61]. A two-stage process was observed: (1) nucleus formation, under the action of attractive capillary immersion forces; and (2) crystal growth, through convective particle flux caused by the water evaporation from the already ordered array (see Fig. 4a). It was shown that one can produce ordered mono- and multilayers of particles by appropriate control of the shape of the liquid film surface and of the water evaporation rate [60]. The term 'convective assembly' was introduced [59] to identify this mechanism of particle ordering under the action of capillary immersion force and hydrodynamic drag force.

During the last few years, the method of convective assembly has found a wide application, see Section 4.6. Ordered arrays from various nano- and micron-sized particles were obtained [62−72$^{\bullet\bullet}$,73,74$^{\bullet}$, 75,76$^{\bullet}$,77−81] by the method described in Denkov et al. [60,61] or its modifications. Several research groups suggested new versions of equipment or procedures (based on the same principles and governing forces), which were aimed at improving the control or at simplifying the procedures for particle array formation. Thus, Dimitrov and Nagayama [65] developed a set-up which resembles in construction the dip-coating apparatus: by appropriate control of the rates of water evaporation and substrate withdrawal, they suc-
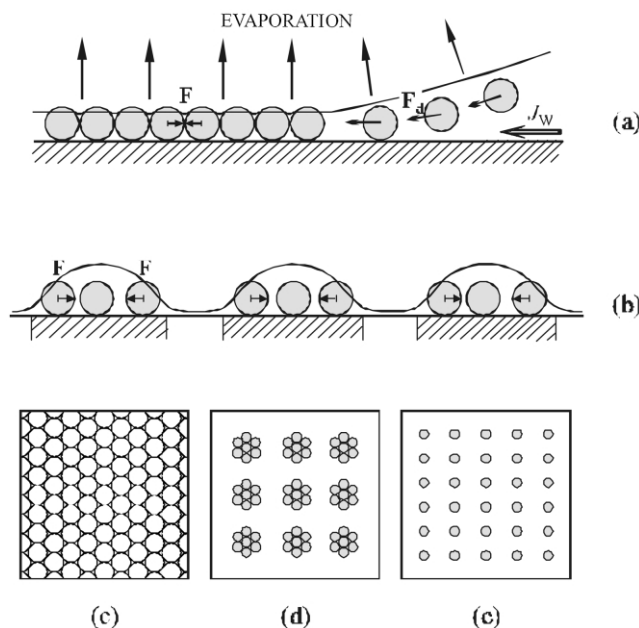
Fig. 4. Ordering of spherical particles in wetting films on substrates: (a) Main driving forces in the convective assembly process: F is a lateral capillary immersion force, between particles captured in the thin liquid film. F_d is a hydrodynamic force, which drags the particles suspended in the thicker layers towards the thinner regions. F_d is caused by a hydrodynamic flux, J_W, which compensates the water evaporated from thinner regions [60,61]. (b) Ordering of particles on patterned solid surfaces. The lateral capillary immersion force, F, acting between particles localised in a given domain, focuses these particles towards the domain center. The conventional method of convective assembly leads to formation of (c) close-packed mono- and multilayers of particles, whereas the assembly on patterned substrates can be used to fabricate (d) small particle clusters or (e) regular arrays of particles with desired lattice shape and separation [85••]. In Qin et al. [88•] the particles are formed in situ in the microdroplets sitting over the hydrophilic domains.

ceeded in obtaining centimetre sized, homogeneous in thickness, ordered arrays of latex particles. Other versions of the method utilise a deposition of the suspension with a plate (playing the role of a brush) or through an extruder [3•,59,68].

In other studies [82], the suspension spreading has been facilitated by applying the spin-coating technique (rotating substrate), which is widely used in the polymer industry for casting polymer films. The quality of the final ordered array can be improved if appropriate agitation by sonication is applied during the film drying process [67]. A relatively simple procedure was introduced by Micheletto et al. [66]: a drop of suspension was placed on a glass plate, which was then tilted at an appropriate angle. The array formation starts at the upper edge of the drop and proceeds downwards. Jiang et al. [72••] proposed an efficient procedure for the formation of large single-crystal colloidal multilayers of silica particles by means of controlled evaporation of the disperse medium and the ensuing action capillary forces.

Experiments with latex particles on mercury substrates confirmed the important role of the immersion capillary forces for the convective assembly process and showed that the electrical potential of mercury can be used as another parameter for control of the particle–substrate interaction and thereby, of the ordering process [3•,59]. One interesting observation in these studies was the size separation of the particles, when mixtures of particles of various sizes were used [1,77]: the larger particles always collected in the centre of the close-packed hexagonal cluster, surrounded by smaller particles. The reason for this segregation is that the larger particles are pressed by the film surface and start attracting each other by capillary immersion forces before the smaller particles.

It was demonstrated [78] that another liquid, perfluorinated oil, can be used as a sub-phase for convective particle assembly. The advantages of the liquid substrates (molecular smoothness and mobility of their surfaces) were discussed in relation to the quality of the final ordered arrays. The optical-microscope observations [78] showed that the process is governed by the same forces as in the case of solid substrate: the immersion–capillary and hydrodynamic–drag forces.

Several studies [48•,79–81] showed that the convective assembly method is operative even for particles, which are captured in free-standing (foam) films. Therefore, the solid or liquid substrates are not a necessary component of the assembly process, because the liquid film itself acts as a 2D matrix for particle packing. Following this approach Denkov et al. [79–81] developed a new procedure for the preparation of vitrified aqueous films, which contain mono- or multi-layers of particles, suitable for electron cryo-microscopy [83]. The method was applied to nanometre sized latex particles and to monodisperse vesicles made of a lipid–protein mixture.

4.2. Self-assembly of particles on patterned substrates or in capillary networks

During the last years, several new approaches to the particle self-assembly into complex 2D structures have emerged. One way to fabricate such structures is to use a solid substrate, whose surface is chemically patterned, e.g. by the microcontact printing method [84], so that different domains of desired shape and size are formed. Aizenberg et al. [85••] showed that micro-patterned substrates, bearing cationic and anionic regions, can be utilised. The particles preferentially stick to the domains of the opposite electric charge. Next, the substrate is rinsed with water, thus removing the non-attached particles. After the rinsing, one observes that the attached particles are con-

tained in residual water droplets (Fig. 4b). Upon evaporation of water, each droplet compresses the particles towards the domain centre leaving an ordered cluster after drying is complete. By this procedure, very well ordered 2D particle arrays of desired symmetry and lattice constant (which could be much larger than the particle diameter) were produced [85••]. Furthermore, small clusters of 5 to 7 particles were assembled in the nodes of a 2D periodic lattice (Fig. 4d).

It was demonstrated that other types of particle−surface interactions can be used to induce a deposition of particles onto patterned substrates [86,87]. One can conclude that this method for the formation of complex structures has a big potential for further development and applications. An interesting modification of this technique was suggested by Qin et al. [88•] and Zhong et al. [89] who used micro-droplets, formed on the hydrophilic domains of the patterned substrate (similar to those described above [85••]), as micro-crystallisation or micro-chemical reactors, in which the particles were formed in situ, during the drying process. Thus, well ordered arrays of micro- and nano-particles were formed with lattice geometry and spacing, which replicated the initial pattern. In this technique, the particle size and lattice constant can be conveniently controlled by varying the domain size and the concentration of the initial suspension.

There are experimental indications that the capillary forces play some role in the deposition of micelles on solid surfaces [90,91]. Massay et al. [90] succeeded to orient specially designed core−shell micelles of a cylindrical shape along nano-sized grooves, created by electron beam lithography and reactive ion etching on the surface of a silicon wafer. Thus, nanoscopic lines of approximately 3 nm in height and 15 nm in width were formed, which followed the contours of the lithographic grooves.

A different approach to the formation of complex 2D and 3D structures of ordered micro-spheres in pre-formed templates was proposed by Kim et al. [92••]. First, a PDMS stamp is produced, whose surface has a relief of micro-channels of the desired shape and connectivity. This stamp is placed over a solid support and the formed network of micro-capillaries is set in contact with a suspension of latex particles. The capillaries spontaneously suck-in suspension and close-packed 2D and 3D arrays of particles are found to fill-up the micro-channels under appropriate conditions. It should be noted that the ordering of the latex particles in these experiments is not driven by capillary forces. The authors showed [92••] that the particles pack in the micro-capillaries mainly under the action of a hydrodynamic drag force, created by the water evaporation at the capillary exits,

which resembles the analogous process in the convective assembly method [60,61]. The term MIMIC (micro-moulding in capillaries) is used to name this technique [92••]. The latter can be applied to a variety of liquids, which solidify (or which contain a substance able to solidify) upon the appropriate treatment: polymerisation, curing, crystallisation, etc. Thus, a solid micro-pattern of complex structure can be formed from various materials in the capillaries. The removal of the PDMS stamp results in a patterned substrate. A further chemical or physical treatment can be used to detach the pattern from the support and to obtain free-standing structures. Formations of polyurethane (free-standing or attached to Si/SiO_2 substrate), various salts (KH_2PO_4, $CuSO_4$, $K_3Fe(CN)_6$ and others), silica and metals were fabricated by means of the MIMIC procedure [92••]. A rich variety of patterns can be produced using this relatively simple method.

Following a similar idea, Park et al. [93•] obtained large crystalline assemblies of particles by injecting latex suspension, under pressure, in a narrow slit between two planar surfaces. Micro-channels were made in one of the side-walls of the slit, so that the fluid was able to flow through these channels under the action of the applied pressure. The channels were smaller in size than the diameter of the latex particles, therefore the latter remained captured in the slit. By optimising the applied pressure, water evaporation rate and intensity of sonication, perfectly ordered crystalline assemblies of various thickness were fabricated.

Capillary immersion forces could be involved in the observed formation of close-packed arrays of nanoparticles in condensed alkylamine films [94,95]. The role of the meniscus, mediating the capillary interaction, can be played by amphiphilic bilayers, which probably form in the structured alkylamine films.

A comprehensive review on various unconventional techniques for fabricating complex nanostructures was recently published by Xia et al. [96].

4.3. Self-assembly of non-spherical objects into 2D arrays

In the framework of the so-called meso-scale self-assembly (MESA) project, Whitesides et al. [40,41••, 97−102••] developed a new procedure for the fabrication of complex 2D structures from millimetre and sub-millimetre sized plates floating on the interface between water and perfluorodecalin. The plates were made of PDMS moulds of desired shape (square, hexagon, hexagonal rings, or more complex) and their side walls were selectively rendered hydrophobic or hydrophilic. By addition of aluminium oxide to the PDMS mould, the authors were able to vary the mass

density of the plates between that of water (1 g/cm^3) and perfluorodecalin (1.9 g/cm^3). Depending on the mass of the plates and on the hydrophobicity/hydrophilicity of their side walls, lateral capillary forces of different sign and magnitude appear between the neighbouring sides of two approaching plates: some of the sides repel, while others attract each other. As a result, the plates acquire an optimal mutual orientation, which minimises the overall free energy of the system. A shape selective, lock-and-key mechanism is imposed in this way. Taking into account the millimetre size of the plates and the different wettability of their side walls, one can realise that the lateral capillary forces in these systems presents a combination of the flotation force, driven by gravity (Fig. 1b), with the immersion force between the 'capillary multipoles' (Fig. 1e).

By using a mild agitation (oscillatory rotation of the container with controlled amplitude and frequency), the authors were able to balance the capillary interaction with the disrupting hydrodynamic shear force, so that well ordered arrays were generated. Whitesides et al. [40,41••,97−102••] were able to produce in this way a large variety of complex structures: 2D close-packed or porous (open) arrays; linear oligomer- and polymer-like aggregates from similar or complementary in shape (lock-and-key) plates; closed rings of given size and shape; polymer-like branched aggregates; and many others (Fig. 3a,b,c,d). The observed shape-selective recognition and self-assembly were qualitatively explained by the local deformation of the meniscus around each side of the plates, which gives rise to lateral capillary forces. A far reaching analogy with the receptor−ligand interactions in chemistry was drawn and the term 'capillary bonds' was introduced to designate this type of directed capillary interaction. One can envisage a virtually unlimited variety of hierarchical structures that can be obtained by the MESA approach.

The attempts to reduce the characteristic size of the plates down to a micrometer size resulted in less ordered arrays, in which the density of defects was higher [101]. This result was attributed to two main reasons: (i) the reduced magnitude of the buoyancy force, which affects the deformation of the fluid interface and thereby the flotation force; and (ii) the reduced magnitude of the hydrodynamic shear forces, imposed by the oscillatory motion, for the smaller particles. The second problem could be probably be overcome by using some other means of system agitation (e.g. sonication). The first problem, however, recalls the necessity for a more rigorous scaling of the magnitude of capillary forces acting between such shaped objects having neither rotational nor translational symmetry; a corresponding theory is still missing.

The MESA approach was successfully applied for fabrication of complex 3D structures as well. By using the surface of a suspended emulsion drop (water-in-oil or oil-in-water) as a template, a self-assembled, virus-like shell was formed from gold hexagonal rings with size of approximately 100 μm [103•]. To prevent the shell disassembly upon drying, the authors deposited a thin silver layer over the ordered hexagonal rings by using a micro-electrode. The electro-deposition welded the rings into a spherical assembly, which was sufficiently robust to withstand the strong capillary forces upon drying and to remain intact in air. This is one of the most complex tailored procedures, involving a stage of particle self-assembly under the action of lateral capillary forces, which has so far been realised. A simpler version of this technique was first suggested by Velev et al. [104,105], who ordered micrometer sized latex beads on the surface of emulsion drops.

4.4. Formation of balls and rings of structured spherical particles

Recently Velev et al. [106••] developed a new procedure for assembly of micro- and nano-particles into free-standing, millimetre-sized ordered structures of various shapes. Aqueous droplets of colloidal suspension were placed on the surface of an inert liquid substrate (perfluoromethyldecalin). The slow evaporation of water led to shrinking of the aqueous drops and to a gradual concentration of the suspended particles. Eventually, a compact 3D colloid crystal was formed. The shape and size of the final assembly can be controlled by various factors, such as the size of the initial drop, particle concentration and presence of surfactants. The latter affect the interfacial tensions (and thereby the shape of the drop) and the appearance of hydrodynamic fluxes, as a result of the surfactant-driven Marangoni effect during evaporation. By appropriate control of the conditions, Velev et al. [106••] obtained spherical, discoidal, dimpled and toroidal (ring-shaped) assemblies. Anisotropic assemblies were obtained by using mixtures of magnetic + non-magnetic or plastic + gold particles. This method seems rather versatile and can be applied to a wide variety of inorganic and plastic particles and their mixtures.

Rings of particles, deposited on solid substrates, are often observed after drying of suspension drops on solid substrates [60,107−109]. The optical observations and the theoretical models have shown that the prevailing force, which determines the particle transport and arrangement in these systems, is the hydrodynamic drag force, caused by the liquid evaporation [60,61]. The ring formation in these experiments is explained by the following scenario [60,107−109]:

firstly, some of the particles irreversibly stick to the substrate at the three-phase contact line (drop periphery) under the action of normal capillary force. The stuck particles pin the contact line so that the process proceeds at a fixed contact radius. The liquid evaporation from the edge is compensated by liquid flow from the interior, which drags the suspended particles towards the drop periphery (Fig. 5a). As a result, most of the particles get accumulated in the region of the contact line and are compressed there by the liquid meniscus at the final stage of drying. The ring size in these experiments is determined by the initial radius of the contact line. Therefore, this method can be further developed by depositing suspension drops on well defined lattice domains on patterned substrates, similar to those described in the Section 4.3 [84,85●●,86−88●,89]. In this way, well ordered arrays of rings of given size could be fabricated in a controlled manner.

Ohara et al. [110,111] studied the formation of submicrometer rings upon drying of wetting films containing very small nanoparticles (3−5 nm in diameter). A characteristic feature of this system is that the particles are so small, that various surface forces become operative in the wetting film of thickness comparable to the particle diameter. These surface forces may induce film destabilisation and hole formation. Therefore, the authors Ohara and Gelbart, and Ohara et al. [110,111] have hypothesised that the particulate rings in their experiments are formed as a result of the nucleation and expansion of holes in the wetting film at the final stage of its drying. The rim of the expanding hole drags the particles away and arranges them into annular rings (Fig. 5b). The effects

of solvent evaporation and surface forces on the conditions for hole nucleation were studied [110].

4.5. The 2D clusters and foam-like formations of particles on a fluid interface

Several studies [51●●,112−115●,116●,117,118] reported the formation of 2D clusters and foam-like structures from micrometer-sized spherical particles on the air−water interface. The interparticle spacing in these arrays was about several particle diameters. The structuring was observed after spreading a drop of suspension over the surface of an aqueous subphase. In some of these studies, the results can be explained either by pure electrostatic repulsion between the particles [114,115●], or by an interplay of the common flotation capillary force (Fig. 1b) with the van der Waals and electrostatic forces [112,113].

Other observations [51●●,116●,117,118], however, required the authors to invoke a very long-range attraction between the particles. This could be neither the van der Waals force (which was negligible at such separations) nor the flotation capillary force, because the particles were too small and the respective interaction energy was well below the thermal energy, kT. It is worthwhile noting that in these experiments the disperse medium of the suspension, used for spreading of the latex particles, was a methanol/water mixture (9/1). Stamou et al. [51●●] suggested that the governing, long-range attractive force in the latter experiments is created by nano-scopic irregularities of the three-phase contact line, i.e. by immersion force between 'capillary multipoles' (Fig. 1e) and developed a respective theoretical model. One should note, however, that the observed evolution from 2D foam to 2D clusters in these experiments resembles very much the processes observed when an aqueous suspension of latex particles was spread over liquid perfluorodecalin sub-phase [78]. Observations in reflected light of the particle assembly process on perfluorodecalin proved that the latex particles were captured in thin aqueous films [78] and the assembly process was driven by the immersion force between 'capillary charges', which is sufficiently strong and long-ranged to explain the observed phenomena. Therefore, it is worthwhile verifying whether some oily film (say from dissolved styrene oligomers) is not generated on the surface of the aqueous sub-phase when spreading the suspension of latex particles in methanol.

4.6. Applications of 2D particle arrays

Here we briefly overview the main areas, in which the 2D colloidal arrays, assembled with the help of capillary forces, find application.
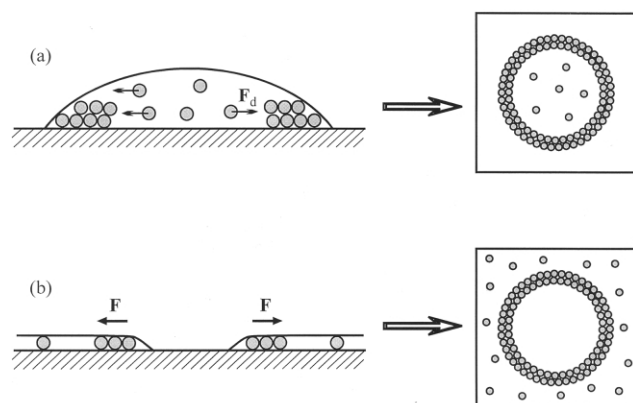

Fig. 5. Two possible ways for fabrication of circular particulate rings on substrates: (a) by evaporating drops of suspensions; in this case the particle transport is driven by a hydrodynamic drag force, F_d. (b) By hole formation and subsequent expansion, which leads to lateral capillary immersion force at the rim periphery. The simultaneous formation of many holes in the layer leads to formation of 2D foam-like assembly.

The ordered 2D arrays of monodisperse latex particles attracted the attention of researchers a long time ago due to their interesting optical properties [54,62,72••,73,74•,119,120•,121–123]. When the particle size and spacing are comparable to the wavelength of the illuminating light, a rich variety of optical phenomena, caused by the light diffraction and interference can be observed. Since the lattice constant and the refractive index of the particles can be varied in wide ranges, the optical properties of the arrays can be finely tuned. Therefore, the 2D colloid crystals are studied in the literature as optical elements, such as diffraction gratings, interference filters, antireflection coatings, micro-lenses, etc. [54,62,72••,119]. Along with these more conventional applications, recent studies were directed to study the application of particle arrays as basic photonic elements and as photonic band-gap crystals, i.e. as periodic dielectric structures, in which the photons behave in a manner similar to that of electrons in semiconductors [73,74•,120•, 121–123].

During the last several years rapid progress was achieved in developing procedures for fabrication of regular, highly porous structures from various materials by using 2D and 3D colloid crystals as templates [124–127•,128•,129,130•,131,132]. Such porous structures have been obtained from inorganic oxides, polymers, glassy carbon, semiconductors and metals. These structures are of great interest due to their unique optical properties and possible applications in catalysis, including the photo- and electro-catalysis. A comprehensive overview on this subject can be found in Holland et al., Jiang et al. and Velev and Kaler [127•,128•,130•].

Ordered 2D particle monolayers were successfully applied as lithographic masks for fabrication of regular nano-structures on silicon substrates by etching or vacuum deposition of metal [75,76•,82,133]. For this purpose, Burmeister et al. [76•] further developed the convective assembly method by including several additional steps: The pre-formed dry 2D array of latex particles was reinforced by vacuum deposition of metal or by thermal annealing. These procedures led to shrinking of the openings between the latex beads, without completely closing them. Afterwards, the glass substrate was slowly dipped into a water bath and the strengthened particle monolayer floated off onto the water surface. If a metal deposition is used, the substrate remains covered with a regular array of nano-metal dots, which replicate the voids between the latex particles in the initial array. However, the floating particle array can be transferred from the water surface onto another solid substrate for further experiments. In this way, a free standing, transportable lithographic mask was produced. This technique has been termed 'natural' [133], 'nanosphere' [82] or 'colloid monolayer lithography' [75,76•]. The use of patterned substrates, allows one to obtain 2D crystal symmetries, which are different from the simple close-packed hexagonal array [76•].

The process of particle ordering in wetting films is related to paint coatings. Recent studies showed [134–136•] that the paint layer formation from aqueous dispersions resembles in some aspects the convective assembly process. In many systems (especially in those containing surfactants) the drying of the paint layer is not uniform but occurs through a moving zone, which separates the wet (thicker) from the dry (thinner) films — this 'compaction' zone moves in the plane of the layer so that the dry regions expand with time at the expense of the wet regions. A hydrodynamic force (caused by the water evaporation) drags the suspended particles from the wet regions towards the dry regions, just as in the convective assembly method [60,61]. This hydrodynamic flux redistributes also the electrolytes and surfactants, so that the final composition of the dry layer is non-uniform in the plane of the layer [134,135]. The degree of particle ordering in the final layer depends primarily on the processes taking place in the compaction zone, where the capillary forces press the particles against each other and against the substrate. The capillary bridge forces play a dominant role also in the process of particle deformation (and to some extent, of particle fusion) in the latex layers [134–136•,137,138].

Ordered monolayers of particles are used also in some biological studies. Thus, Miyaki et al. [139] studied the interaction of neutrophil-type biological cells with particle arrays as a function of the particle size. They found that the contact of the cells with the particle array activated the cell to an extent, which strongly depended on the particle size. Thus, the particle arrays serve as convenient micro-patterned surfaces for studying the cell adhesion. The wide ranges of available particle sizes and compositions, along with the possibility to graft various bio-active molecules onto the particle surface, imply that these studies will expand in the future.

5. Summary and conclusions

The review of publications from the last 2–3 years shows that there is a permanent interest in the various kinds of capillary forces, which often play an essential role in fundamental and applied studies. The capillary bridge forces (Fig. 1a) are investigated in relation to AFM experiments [4–6,8–10•,11,32], studies on capillary condensation and measurements by the surface-force apparatus [18,24–27], capillary cavitation and long-range hydrophobic surface force [23,28–35], antifoaming action of oily drops

[13,14●,15]. The flotation lateral capillary force (Fig. 1b) is employed in surface rheological measurements [38] and for self-assembly of floating meso-scale objects [40,41●●,97−102●●]. The common immersion capillary force (Fig. 1c) is reported to take part in the 2D aggregation and ordering of micrometer-sized and sub-micrometer particles confined in wetting and free-standing liquid films [54−72●,73,74●,75,76●, 77−82].

Systematic presentation of the theory of the aforementioned types of capillary forces (Fig. 1a−c) was recently published [2●,3●]. New theoretical developments are devoted to the description of the immersion force in the case of finite menisci (Fig. 1d) [50●] and the forces between 'capillary multipoles' (Fig. 1e) [51●●]. The latter two themes mark directions for future research, both theoretical and experimental.

The studies on self-assembly of colloidal particles, mediated by the action of capillary forces, develops along the following major directions: improving the procedures for particle assembly in wetting films [72●●] or in shrinking drops [106●●], structuring on patterned substrates or in capillary networks [85●●,86−88●,89,90,92●●], and self-assembly of floating non-spherical objects into complex 2D arrays [41●●,102●●]. The obtained ordered structures of particles have found miscellaneous applications.

Acknowledgements

References and recommended reading

● of special interest
●● of outstanding interest

[1] Yamaki M, Higo J, Nagayama K. Size-dependent separation of colloidal particles in two-dimensional convective self-assembly. Langmuir 1995;11:2975−2978.

[2] Kralchevsky PA, Nagayama K. Capillary interactions
● between particles bound to interfaces, liquid films and biomembranes. Adv. Colloid Interface Sci. 2000;85:145−192.
An overview, comparison and discussion of recent results, both theoretical and experimental, about lateral capillary forces.

[3] Kralchevsky PA, Nagayama K. Particles at fluid interfaces
● and membranes: attachment of colloid particles and proteins to interfaces and formation of two-dimensional arrays. Amsterdam: Elsevier, 2001.
Chapters 7−9: theory and experiment on lateral capillary forces. Chapter 10: interactions between inclusions in lipid membranes. Chapter 11: capillary bridges and capillary-bridge forces. Chapter 12: capillary forces between particles of irregular contact line.

Chapter 13: two-dimensional crystallisation of particulates and proteins. Chapter 14: effect of oil drops and particulates on the stability of foams (antifoaming).

[4] Fujihira M, Aoki D, Okabe Y, Takano H, Hokari H. Effect of capillary force on friction force microscopy: a scanning hydrophilicity microscope. Chemistry Letters, 1996:499−500. (Japan)

[5] Behrend OP, Oulevey F, Gourdon D et al. Intermittent contact: tapping or hammering? Applied Physics A 1998;66:S219−S221.

[6] Suzuki H, Mashiko S. Adhesive force mapping of friction-transferred PTFE film surface. Applied Physics A 1998;66:S1271−S1274.

[7] Fielden ML, Hayes RA, Ralston J. Surface and capillary forces affecting air bubble — particle interactions in aqueous electrolyte. Langmuir 1996;12:3721−3727.

[8] Preuss M, Butt H-J. Direct measurement of particle-bubble interactions in aqueous electrolyte: dependence on surfactant. Langmuir 1998;14:3164−3174.

[9] Preuss M, Butt H-J. Measuring the contact angle of individual colloidal particles. J. Colloid Interface Sci. 1998; 208:468−477.

[10] Ecke S, Preuss M, Butt H-J. Microsphere tensiometry to
● measure advancing and receding contact angles on individual particles. J. Adhesion Sci. Technol. 1999;13:1181−1191.
Silanized silica spheres, 4.1 μm in diameter, were used. The distance to which a sphere, attached to the AFM cantilever, jumps into its equilibrium position at the air-liquid interface of a drop or an air bubble was measured. From these distances the contact angles were calculated. No hysteresis was measured with microspheres, whereas a considerable hysteresis was established with similarly prepared planar silica surfaces.

[11] Preuss M, Butt H-J. Direct measurement of forces between particles and bubbles. Int. J. Miner. Process. 1999;56:99−115.

[12] Aveyard R, Clint JH. Liquid lenses at fluid/fluid interfaces. J. Chem. Soc. Faraday Trans. 1997;93:1397−1403.

[13] Denkov ND, Cooper P, Martin J-Y. Mechanisms of action of mixed solid-liquid antifoams. 1. Dynamics of foam film rupture. Langmuir 1999;15:8514−8529.

[14] Denkov ND. Mechanisms of action of mixed solid-liquid
● antifoams. 2. Stability of oil bridges in foam films. Langmuir 1999;15:8530−8542.
A new, 'bridging-stretching', mechanism of foam destruction by oil drops was proposed based on systematic experimental investigations. The small oil bridges in foam films are stable, whereas the larger bridges are unstable (few milliseconds lifetime). Initially stable small bridges could be later transformed into unstable ones due to the thinning of the foam films and the transfer of pre-spread oil.

[15] Denkov ND, Marinova KG, Christova C, Hadjiiski A, Cooper P. Mechanisms of action of mixed solid-liquid antifoams: 3. Exhaustion and reactivation. Langmuir 2000;16:2515−2528.

[16] Abramowitz M, Stegun IA. Handbook of mathematical functions. New York: Dover, 1965.

[17] Dimitrov AS, Miwa T, Nagayama K. A comparison between the optical properties of amorphous and crystalline monolayers of silica particles. Langmuir 1999;15:5257−5264.

[18] Aveyard R, Clint JH, Paunov VN, Nees D. Capillary condensation of vapours between two solid surfaces: effects of line tension and surface forces. Phys. Chem. Chem. Phys. 1999;1:155−163.

[19] Orr FM, Scriven LE, Rivas AP. Pendular rings between solids: meniscus properties and capillary force. J. Fluid Mech. 1975;67:723−742.

[20] de Lazzer A, Dreyer M, Rath HJ. Particle — surface capillary forces. Langmuir 1999;15:4551−4559.

[21] Kolodezhnov VN, Magomedov GO, Mal'tsev GP. Refined determination of shape for the free surface of the liquid region in analysis of capillary interaction of powder particles. Colloid J. Russ. 2000;62:443−450.

[22] Willett CD, Adams MJ, Johnson SA, Seville JPK. Capillary bridges between two spherical bodies. Langmuir 2000; 16:9396−9405.

[23] Attard P. Thermodynamic analysis of bridging bubbles and a quantitative comparison with the measured hydrophobic attraction. Langmuir 2000;16:4455−4466.

[24] Yaminsky VV. Long range attraction in water vapor. Capillary forces relevant to 'polywater'. Langmuir 1997;13:2−7.

[25] Xiao X, Quian L. Investigation of humidity-dependent capillary force. Langmuir 2000;16:8153−8158.

[26] Claesson PM, Dedinaite A, Bergenståhl B, Campbell B, Christenson H. Interaction between hydrophobic mica surfaces in triolein: triolein surface orientation, solvation forces, and capillary condensation. Langmuir 1997;13:1682−1688.

[27] Petrov P, Olsson U, Wennerström H. Surface forces in bicontinuous microemulsions: water capillary condensation and lamellae formation. Langmuir 1997;13:3331−3337.

[28] Carambassis A, Jonker LC, Attard P, Rutland MW. Forces measured between hydrophobic surfaces due to a submicroscopic bridging bubble. Phys. Rev. Lett. 1998;80: 5357−5360.

[29] Considine RF, Hayes RA, Horn RG. Forces measured between latex spheres in aqueous electrolyte: Non-DLVO behavior and sensitivity to dissolved gas. Langmuir 1999;15:1657−1659.

[30] Considine RF, Drummond CJ. Long-range force of attraction between solvophobic surfaces in water and organic liquids containing dissolved air. Langmuir 2000;16:631−635.

[31] Mahnke J, Stearnes J, Hayes RA, Fornasiero D, Ralston J. The influence of dissolved gas on the interactions between surfaces of different hydrophobicity in aqueous media. Part I. Measurement of interaction forces. Phys. Chem. Chem. Phys. 1999;1:2793−2798.

[32] Yakubov GE, Butt H-J, Vinogradova O. Interaction forces between hydrophobic surfaces. Attractive jump as an indication of formation of 'stable' submicrocavities. J. Phys. Chem. B 2000;104:3407−3410.

[33] Ederth T. Substrate and solution effects on the long-range 'hydrophobic' interactions between hydrophobized gold surfaces. J. Phys Chem. B 2000;104:9704−9712.

[34] Ishida N, Sakamoto M, Miyahara M, Higashitani K. Attraction between hydrophobic surfaces with and without gas phase. Langmuir 2000;16:5681−5687.

[35] Ishida N, Inoue T, Miyahara M, Higashitani K. Nano bubbles on a hydrophobic surface in water observed by tapping-mode atomic force microscopy. Langmuir 2000;16:6377−6380.

[36] Chan DYC, Henry JD, White LR. The interaction of colloidal particles collected at fluid interfaces. J. Colloid Interface Sci. 1981;79:410−418.

[37] Paunov VN. On the analogy between lateral capillary interactions and electrostatic interactions in colloid systems. Langmuir 1998;14:5088−5097.

[38] Petkov JT, Danov KD, Denkov ND, Aust R, Durst F. Precise method for measuring the shear surface viscosity of surfactant monolayers. Langmuir 1996;12:2650−2653.

[39] Petkov JT, Gurkov TD, Campbell BE, Measurement of the yield stress of gel-like protein layers on liquid surfaces by means of an attached particle. Langmuir 2001, 17, in press.

[40] Bowden N, Terfort A, Carbeck J, Whitesides GM. Self-assembly of mesoscale objects into ordered two-dimensional arrays. Science 1997;276:233−235.

[41] Bowden N, Choi IS, Grzybowski BA, Whitesides GM. Mesoscale self-assembly of hexagonal plates using lateral capillary
●●

forces: synthesis using the capillary bond. J. Am. Chem. Soc. 1999;121:5373−5391.

The interactions between floating hexagonal plates, 5.4 mm in diameter, were experimentally examined. The faces of the plates were functionalized to be hydrophilic or hydrophobic; in this way various types of 'capillary multipoles' were realized. The strength and the directionality of the interactions can be tailored by manipulating the geometric size and the pattern of hydrophobization. The type of 2D lattice of the assemblies was investigated as a function of the sort of particles.

[42] Grzybowski BA, Bowden N, Arias F, Yang H, Whitesides GM. Modeling menisci and capillary forces from the millimeter to the micrometer size range. J. Phys. Chem. B 2001;105:404−412.

[43] Kralchevsky PA, Paunov VN, Denkov ND, Nagayama K. Stresses in lipid membranes and interactions between inclusions. J. Chem. Soc. Faraday Trans. 1995;91:3415−3432.

[44] Gil T, Ipsen JH, Mouritsen OG, Sabra MC, Sperotto MM, Zuckermann MJ. Theoretical analysis of protein organization in lipid membranes. Biochim. Biophys. Acta 1998; 1376:245−266.

[45] Mansfield SL, Gotch AJ, Harms GS, Johnson CK, Larive CK. Complementary analysis of peptide aggregation by NMR and time-resolved laser spectrometry. J. Phys. Chem. B 1999;103:2262−2269.

[46] Kralchevsky PA, Paunov VN, Nagayama K. Lateral capillary interaction between particles protruding from a spherical liquid layer. J. Fluid Mech. 1995;299:105−132.

[47] Maenosono S, Dushkin CD, Yamaguchi Y. Direct measurement of the viscous force between two spherical particles trapped in a thin wetting film. Colloid Polym. Sci. 1999;277:993−996.

[48] Velikov KP, Durst F, Velev OD. Direct observation of the
●   dynamics of latex particles confined inside thinning water−air films. Langmuir 1998;14:1148−1155.

Dynamics of micrometer-sized latex particles confined in thinning foam films was investigated. The behavior of the particles depend on several experimental factors, incl. the type of surfactant. In some experiments the captured particles tended to form small 2D aggregates; the latter were observed to attract each other from distances, which could reach up to 100 μm. This attraction was attributed to the lateral immersion force. At higher particle concentration the formation of '2D-foam' structure was observed.

[49] Dietrich C, Angelova M, Pouligny B. Adhesion of latex spheres to giant phospholipid vesicles: statics and dynamics. J. Phys. II Fr. 1997;7:1651−1682.

[50] Danov KD, Pouligny B, Angelova MI, Kralchevsky PA.
●   Strong capillary attraction between spherical inclusions in a multilayered lipid membrane. In: Iwasawa Y, Oyama N, Kunieda H, editors. Amsterdam: Elsevier, 2001.

Strong attraction has been experimentally observed between two spherical latex particles, which are included in the membrane of a giant spherical phospholipid vesicle. This attraction was interpreted as a lateral capillary force resulting from the overlap of the menisci formed around each of the two particles. The theoretical results about the force are in line with the experimentally observed trends.

[51] Stamou D, Duschl C, Johannsmann D. Long-range attraction
●●   between colloidal spheres at the air-water interface: the consequence of an irregular meniscus. Phys. Rev. E 2000;62:5263−5272.

Theory of the interactions between floating spherical particles with undulated contact line ('capillary multipoles') is developed. A convenient analytical expression is obtained for the energy of interaction between two capillary quadrupoles. Frustrations of the formation of some types of 2D lattices due to inadequate particle

orientations are discussed. The theoretical predictions are compared with experimental data for structuring of latex particles spread over the surface of water.

[52] Lucassen J. Capillary forces between solid particles in fluid interfaces. Colloids Surf. 1992;65:131–137.

[53] Petkov JT, Gurkov TD, Campbell BE, Borwankar RP. Dilatational and shear elasticity of gel-like protein layers on air/water interface. Langmuir 2000;16:3703–3711.

[54] Alfrey Jr. T, Bradford EB, Vanderhof JW, Oster G. Optical properties of uniform particle-size latexes. J. Optical Soc. Am. 1954;44:603–609.

[55] Vanderhoff JW, Bradfod EB, Carrington WK. The transport of water through latex films. J. Polymer Sci. Symp. 1973; 41:155–174.

[56] Horne RW. The formation of virus crystalline and paracrystalline arrays for electron microscopy and image analysis. Adv. Virus Res. 1979;24:173–221.

[57] Harris JR. The negative staining-carbon film procedure: technical considerations and a survey of macromolecular applications. Micron Microscopica Acta 1991;22:341–359.

[58] Yoshimura H, Matsumoto M, Endo S, Nagayama K. Two-dimensional crystallization of proteins on mercury. Ultramicroscopy 1990;32:265–274.

[59] Nagayama K. Two-dimensional self-assembly of colloids in thin liquid films. Colloids Surfaces A 1996;109:363–374.

[60] Denkov ND, Velev OD, Kralchevsky PA, Ivanov IB, Yoshimura H, Nagayama K. Mechanism of formation of two-dimensional crystals from latex particles on substrates. Langmuir 1992;8:3183–3190.

[61] Denkov ND, Velev OD, Kralchevsky PA, Ivanov IB, Yoshimura H, Nagayama K. Two-dimensional crystallization. Nature 1993;361:26.

[62] Dushkin CD, Nagayama K, Miwa T, Kralchevsky PA. Colored multilayers from transparent submicrometer spheres. Langmuir 1993;9:3695–3701.

[63] Dushkin CD, Lazarov GS, Kotsev SN, Yoshimura H, Nagayama K. Effect of growth conditions on the structure of two-dimensional latex crystals: experiment. Colloid Polym. Sci. 1999;277:914–930.

[64] Maenosono S, Dushkin CD, Yamaguchi Y, Nagayama K, Tsujii Y. Effect of growth conditions on the structure of two-dimensional latex crystals: modeling. Colloid Polym. Sci. 1999;277:1152–1161.

[65] Dimitrov AS, Nagayama K. Continuous convective assembling of fine particles into two-dimensional arrays on solid surfaces. Langmuir 1996;12:1303–1311.

[66] Micheletto R, Fukuda H, Ohtsu M. A simple method for the production of two-dimensional, ordered array of small latex particles. Langmuir 1995;11:3333–3336.

[67] Sasaki M, Hane K. Ultrasonically facilitated two-dimensional crystallization of colloid particles. J. Appl. Phys. 1996; 80:5427–5431.

[68] Matsushita S, Miwa T, Fujishima A. Distribution of components in composite two-dimensional arrays of latex particles and evaluation in terms of the fractal dimension. Langmuir 1997;13:2582–2584.

[69] Picard G. Fine particle 2D-crystals prepared by dynamic thin laminar flow method. Langmuir 1997;13:3226–3234.

[70] Du H, Chen P, Liu F, Meng F-D, Li T-J, Tang X-Y. Preparation and assembly of nanosized polymer latex. Mater. Chem. Phys. 1997;51:277–282.

[71] Cardoso AH, Leite CAP, Zaniquelli MED, Galembeck F. Easy polymer latex self-assembly and colloidal crystal formation: the case of poly[styrene-*co*-(2-hydroxyethyl methacrylate)]. Colloids Surf. A 1998;144:207–217.

[72] Jiang P, Bertone JF, Hwang KS, Colvin VL. Single crystal

•• colloidal multilayers of controlled thickness. Chem. Mater. 1999;11:2132–2140.

A new efficient procedure for assembling silica spheres into single-crystal colloid layer, under the action of capillary forces, is described. The method relies on a controlled evaporation of the liquid from a thin suspension layer spread over smooth solid substrate. The thickness of the final particulate layer is determined by the particle concentration in the initial suspension layer. The dependence of the optical properties of the layers on their thickness and particle diameter is studied.

[73] Zhao Y, Avrutsky I. Two-dimensional colloidal crystal corrugated waveguides. Optics Lett. 1999;24:817–819.

[74] Zhao Y, Avrutsky I, Li B. Optical coupling between
• monocrystalline colloidal crystals and a planar waveguide. Appl. Phys. Lett. 1999;75:3596–3598.

The optical properties of the structure 'planar wave-guide/2D colloid crystal' are studied and discussed with respect to possible applications in optical elements.

[75] Burmeister F, Schäfle C, Keilhofer B, Bechinger C, Boneberg J, Leiderer P. From mesoscopic to nanoscopic surface structures: lithography with colloid monolayers. Adv. Mater. 1998;10:495–497.

[76] Burmeister F, Badowsky W, Braun T, Wieprich S, Boneberg
• J, Leiderer P. Colloid monolayer lithography-a flexible approach for nanostructuring of surfaces. Appl. Surface Sci. 1999;144/145:461–466.

Two new, more advanced procedures for application of particle monolayers as lithographic masks are described and discussed.

[77] Antonietti M, Hartmann J, Neese M, Seifert U. Highly ordered size-dispersive packings of polydisperse microgel spheres. Langmuir 2000;16:7634–7639.

[78] Lazarov GS, Denkov ND, Velev OD, Kralchevsky PA, Nagayama K. Formation of two-dimensional structures from colloid particles on fluorinated oil substrate. J. Chem. Soc. Faraday Trans. 1994;90:2077–2083.

[79] Denkov ND, Yoshimura H, Nagayama K, Kouyama T. Nanoparticle arrays in freely suspended vitrified films. Phys. Rev. Lett. 1996;76:2354–2357.

[80] Denkov ND, Yoshimura H, Nagayama K. Method for controlled formation of vitrified films for cryo-electron microscopy. Ultramicroscopy 1996;65:147–158.

[81] Denkov ND, Yoshimura H, Kouyama T, Walz J, Nagayama K. Electron cryomicroscopy of Bacteriorhodopsin vesicles: Mechanism of vesicle formation. Biophys. J. 1998;74: 1409–1420.

[82] Hulteen JC, van Duyne RP. Nanosphere lithography-a materials general fabrication process for periodic particle array surfaces. J. Vac. Sci. Technol. A 1995;13:1553–1558.

[83] Almgren M, Edwards K, Karlsson G. Cryo transmission electron microscopy of liposomes and related structures. Colloids Surf. A 2000;174:3–21.

[84] Xia Y, Tien J, Qin D, Whitesides GM. Non-lithographic methods for fabrication of elastomeric stamps for use in microcontact printing. Langmuir 1996;12:4033–4038.

[85] Aizenberg J, Braun PV, Wiltzius P. Patterned colloidal
•• deposition controlled by electrostatic and capillary forces. Phys. Rev. Lett. 2000;84:2997–3000.

Chemically micropatterned solid substrates, with cationic and anionic regions, are used to localize the deposition of charged colloid particles. Direct microscope observations show that the attachment of the particles to wet substrates leads to formation of loose clusters on the oppositely charged regions. The subsequent drying of the substrate leads to compaction of the particles into well ordered clusters under the action of the immersion capillary force.

[86] Lin K, Crocker JC, Prasad V et al. Entropically driven colloidal crystallization on patterned surfaces. Phys. Rev. Lett. 2000;85:1770–1773.

[87] Chen KM, Jiang X, Kimerling LC, Hammond PT. Selective self-organization of colloids on patterned polyelectrolyte templates. Langmuir 2000;16:7825–7834.

[88] Qin D, Xia Y, Xu B, Yang H, Zhu C, Whitesides GM.
• Fabrication of ordered two-dimensional arrays of micro- and nanoparticles using patterned self-assembled monolayers as templates. Adv. Mater. 1999;11:1433–1437.

Drops deposited on the hydrophilic domains of a patterned surface are used as micro-reactors for confined crystallization or precipitation, so that perfectly ordered 2D arrays of micro- and nano-particles are formed on gold substrates. Both the spatial distribution and the dimension of the solid particles can be easily controlled.

[89] Zhong Z, Gates B, Xia Y. Soft lithographic approach to the fabrication of highly ordered 2D arrays of magnetic nanoparticles on the surfaces of silicon substrates. Langmuir 2000;16:10369–10375.

[90] Massey JA, Winnik MA, Manners I et al., Fabrication of oriented nanoscopic ceramic lines from cylindrical micelles of an organometallic polyferrocene block copolymer. J. Am. Chem. Soc. 2001, 123, in press.

[91] Spatz JP, Herzog T, Moßmer S, Ziemann P, Möller M. Micellar inorganic-polymer hybrid systems — a tool for nanolithography. Adv. Mater. 1999;11:149–153.

[92] Kim E, Xia Y, Whitesides GM. Micromolding in capillaries:
•• applications in materials science. J. Am. Chem. Soc. 1996;118:5722–5731.

A versatile process for fabricating microstructures of polymers, ceramics, metals and microparticles is described. A network of interconnected channels is formed by using a PDMS stamp. An appropriate precursor liquid (or particle suspension) spontaneously penetrates the channels under the action of a capillary suction pressure. The solidifying of the material in the channels and the subsequent stamp removal results in a patterned substrate or in a free-standing film with structure complementary to that of the stamp.

[93] Park SH, Qin D, Xia Y. Crystallization of mesoscale particles
• over large areas. Adv. Mater. 1998;10:1028–1032.

A new procedure for fabrication of relatively large crystalline layers of colloid particles is described. The particles are close-packed in a slit formed between two glass plates under the action of a hydrodynamic drag force. Sonication of the sample is used during the ordering process to improve the crystal quality.

[94] Patil V, Malvankar RB, Sastry M. Role of particle size in individual and competitive diffusion of carboxylic acid derivatized colloidal gold particles in thermally evaporated fatty amine films. Langmuir 1999;15:8197–8206.

[95] Patil V, Sastry M. Formation of close-packed silver nanoparticle multilayers from electrostatically grown octadecylamine/colloid nanocomposite precursors. Langmuir 2000;16:2207–2212.

[96] Xia Y, Rogers AJ, Paul KE, Whitesides GM. Unconventional methods for fabricating and patterning nanostructures. Chem. Rev. 1999;99:1823–1848.

[97] Choi IS, Bowden N, Whitesides GM. Shape-selective recognition and self-assembly of mm-scale components. J. Am. Chem. Soc. 1999;121:1754–1755.

[98] Choi IS, Bowden N, Whitesides GM. Macroscopic, hierarchical, two-dimensional self-assembly. Angew. Chem. Int. Ed. 1999;38:3078–3081.

[99] Wu H, Bowden N, Whitesides GM. Selectivities among capillary bonds in mesoscale self-assembly. Appl. Phys. Lett. 1999;75:3222–3224.

[100] Oliver SRJ, Bowden N, Whitesides GM. Self-assembly of hexagonal rod arrays based on capillary forces. J. Colloid Interface Sci. 2000;224:425–428.

[101] Bowden N, Arias F, Deng T, Whitesides GM. Self-assembly of microscale objects at a liquid/liquid interface through lateral capillary forces. Langmuir 2001;17:1757–1765.

[102] Bowden N, Oliver SRJ, Whitesides GM. Mesoscale self-as-
•• sembly: capillary bonds and negative menisci. J. Phys. Chem. 2000;104:2714–2724.

A systematic experimental investigation of the possible structures formed by a self-assembly of hexagonal plates at the interface between perfluorodecalin and water is performed. All 14 different hexagons that can be made by permuting the number and location of the hydrophobic and hydrophilic side faces were examined. The role of the plate mass density (which affects the shape of the meniscus and thereby the lateral capillary force) is also discussed. Complements reference [41••].

[103] Huck WTS, Tien J, Whitesides GM. Three-dimensional
• mesoscale self-assembly. J. Am Chem. Soc. 1998;120: 8267–8268.

A tailored procedure, including a stage of particle assembly on the surface of an emulsion drop under the action of lateral capillary force between multipoles, was applied to produce a closed spherical shell of metal hexagonal rings (viral-type structure). This assembly was reinforced by electrodeposition, so that the final aggregate was sufficiently strong to sustain drying and to remain intact in air.

[104] Velev OD, Furusawa K, Nagayama K. Assembly of latex particles by using emulsion droplets as templates. 1. Microstructured hollow spheres. Langmuir 1996;12:2374–2384.

[105] Velev OD, Furusawa K, Nagayama K. Assembly of latex particles by using emulsion droplets as templates. 2. Ball-like and composite aggregates. Langmuir 1996;12:2385–2391.

[106] Velev OD, Lenhoff AM, Kaler EW. A class of microstruc-
•• tured particles through colloidal crystallization. Science 2000;287:2240–2243.

A new method for fabrication of highly ordered, microstructured materials is described. A drop of aqueous suspension, floating on the surface of fluorinated oil, is used as a template, in which 3D-colloid crystal is formed. The crystallization is induced by the shrinking surface of the aqueous drop (as a result of a controlled water evaporation), which imposes a capillary force compressing the particles against each other. Particle assemblies with spherical, ellipsoidal and toroidal shape were produced.

[107] Deegan RD, Bakajin O, Dupont TF, Huber G, Nagel SR, Witten TA. Capillary flow as the cause of ring stains from dried liquid drops. Nature 1997;389:827–829.

[108] Uno K, Hayashi K, Hayashi T, Ito K, Kitano H. Particle adsorption in evaporating droplets of polymer latex dispersions on hydrophilic and hydrophobic surfaces. Colloid Polym. Sci. 1998;276:810–815.

[109] Maenosono S, Dushkin CD, Saita S, Yamaguchi Y. Growth of a semiconductor nanoparticle ring during the drying of a suspension droplet. Langmuir 1999;15:957–965.

[110] Ohara PC, Gelbart WM. Interplay between hole instability and nanoparticle array formation in ultrathin liquid films. Langmuir 1998;14:3418–3424.

[111] Ohara PC, Heath JR, Gelbart WM. Self-assembly of submicrometer rings of particles from solutions of nanoparticles. Angew. Chem. Int. Ed. Engl. 1997;36:1078–1080.

[112] Onoda GY. Direct observation of two-dimensional dynamic clustering and ordering with colloids. Phys. Rev. Lett. 1985;55:226–229.

[113] Hórvölgyi Z, Németh S, Fendler JH. Monoparticulate layers of silanized glass spheres at the water-air interface: particle-particle and particle-subphase interactions. Langmuir 1996;12:997–1004.

[114] Aveyard R, Clint JH, Nees D, Paunov VN. Compression and structure of monolayers of charged latex particles at air-water and octane-water interfaces. Langmuir 2000;16: 1969–1979.

[115] Aveyard R, Clint JH, Nees D, Quirke N. Structure and
• collapse of particle monolayer under lateral pressure at the octane/aqueous surfactant solution interface. Langmuir 2000;16:8820–8828.
The structure and collapse of particle monolayers, spread on the octane/water interface, is studied in a modified Langmuir trough. It is proven experimentally that the layers collapse by buckling, when the particle-particle repulsive force (per unit length) becomes equal to the tension of the fluid interface.

[116] Ruiz-Garcia J, Gámez-Corrales R, Ivlev BI. Foam and clus-
• ter structure formation by latex particles at the air/water interface. Physica A 1997;236:97–104.
The formation of 2D foam and cluster structures by latex particles spread over aqueous sub-phase was reported. The unusual observation here was the large interparticle separation, which implies the presence of a very long-range attractive force. The authors explained their results with the interplay of electrostatic repulsion and van der Waals attraction, but the theoretical estimates suggest that probably lateral capillary force (between multipoles [51••] or of immersion type [48•,78]) could be involved in this phenomenon.

[117] Ruiz-Garcia J, Gámez-Corrales R, Ivlev BI. Formation of two-dimensional colloidal voids, soap froths, and clusters. Phys. Rev. E 1998;58:660–663.

[118] Ghezzi F, Earnshaw JC. Formation of meso-structures in colloidal monolayers. J. Phys.: Condens. Matter 1997;9: L517–L523.

[119] Hayashi S, Kumamoto Y, Suzuki T, Hirai T. Imaging by polystyrene latex particles. J. Colloid Interface Sci. 1991; 144(2):538–547.

[120] Matsushita SI, Yagi Y, Miwa T, Tryk DA, Koda T, Fu-
• jishima A. Light propagation in composite two-dimensional arrays of polystyrene spherical particles. Langmuir 2000;16:636–642.
2D colloid crystals, with single fluorescent particles incorporated as light sources, were produced, and the light propagation inside these structures was studied. Two modes of light propagation are distinguished-one propagating inside the particles and another one, caused by the field of the evanescent wave outside the particle surface. The relative contribution of these two modes depends on the ratio particle size/light wavelength.

[121] Yagi Y, Matsushita SI, Tryk DA, Koda T, Fujishima A. Observation of light propagation in single layers of composite two-dimensional arrays. Langmuir 2000;16:1180–1184.

[122] Park SH, Xia Y. Assembly of mesoscale particles over large areas and its application in fabricating tunable optical filters. Langmuir 1999;15:266–273.

[123] Yamasaki T, Tsutsui T. Spontaneous emission from fluorescent molecules embedded in photonic crystals consisting of polystyrene microspheres. Appl. Phys. Lett. 1998;72 (16):1957–1959.

[124] Velev OD, Jede TA, Lobo RF, Lenhoff AM. Porous silica via colloidal crystallization. Nature 1997;389:447–448.

[125] Velev OD, Jede TA, Lobo RF, Lenhoff AM. Microstructured porous silica obtained via colloidal crystal templates. Chem. Mater. 1998;10:3597–3602.

[126] Holland BT, Blanford CF, Stein A. Synthesis of macroporous minerals with highly ordered three-dimensional arrays of spheroidal voids. Science 1998;281:538–540.

[127] Holland BR, Blanford CF, Do T, Stein A. Synthesis of
• highly ordered, three-dimensional, macroporous structures of amorphous or crystalline inorganic oxides, phosphates, and hybrid composites. Chem. Mater. 1999;11:795–805.
Highly ordered, porous oxides of Si, Ti, Zr, Al, W, Fe, Sb, and Zr/Y mixture, were produced from metal alkoxide precursors templated around latex spheres, which were assembled in a 3D colloid crystal. Depending on the conditions during the subsequent calcination, amorphous or crystal forms of these oxides were obtained. Aluminophosphates and silicates, whose surface was grafted with organic molecules, were also produced.

[128] Jiang P, Hwang KS, Mittelman DM, Bertone JF, Colvin VL.
• Template-directed preparation of macroporous polymers with oriented and crystalline arrays of voids. J. Am. Chem. Soc. 1999;121:11630–11637.
A versatile procedure for production of highly porous polymer membranes with periodic regular structure, by using silica colloid crystals as templates, is described. The optical properties of these membranes are studied and their possible applications in optics and separation technologies are discussed.

[129] Velev OD, Tessier PM, Lenhoff AM, Kaler EW. A class of porous metallic nanostructures. Nature 1999;401:548.

[130] Velev OD, Kaler EW. Structured porous materials via col-
• loidal crystal templating: from inorganic oxides to metals. Adv. Mater. 2000;12:531–534.
A concise and comprehensive review on the various procedures for fabrication of structured porous materials by using colloidal crystals as templates. The potential applications of these materials are briefly outlined.

[131] Tessier PM, Velev OD, Kalambur AT, Rabolt JF, Lenhoff AM, Kaler EW. Assembly of gold nanostructured films templated by colloidal crystals and use in surface-enhanced Raman spectroscopy. J. Am. Chem. Soc. 2000;122: 9554–9555.

[132] Wijnhoven JEGJ, Zevenhuizen SJM, Hendriks MA, Van-maekelbergh D, Kelly JJ, Vos WL. Electrochemical assembly of ordered macropores in gold. Adv. Mater. 2000;12: 888–890.

[133] Deckman HW, Dunsmuir JH, Garoff S, Mchenry JA, Peiffer DG. Macromolecular self-organized assemblies. J. Vac. Sci. Technol. B 1988;6:333–336.

[134] Winnik MA. The formation and properties of latex films. In: Lovell PA, El-Aasser MS, editors. Emulsion Polymerization and Emulsion Polymers. New York: Wiley, 1997:468–518.

[135] Winnik MA. Latex film formation. Curr. Opinion Colloid Interface Sci. 1997;2:192–199.

[136] Keddie JL. Film formation of latex. Mater. Sci. Eng.
• 1997;21:101–107.
A comprehensive review on the mechanisms of film formation by latex particles with detailed and analytical account of the various experimental methods and results.

[137] Visschers M, Laven J, German AL. Current understanding of the deformation of latex particles during film formation. Prog. Org. Coating 1997;30:39–49.

[138] Du Chesne A, Bojkova A, Stöckelmann E, Krieger S, Held-mann C. Determining the compacting of latex films upon drying by interference measurements — an approach for the investigation of film formation. Acta Polym. 1998;49: 346–355.

[139] Miyaki M, Fujimoto K, Kawaguchi H. Cell response to micropatterned surfaces produced with polymeric microspheres. Colloids Surf. A 1999;153:603–608.